

Intrinsic Differences in Adipocyte Precursor Cells From Different White Fat Depots

Yazmín Macotela, Brice Emanuelli, Marcelo A. Mori, Stephane Gesta, Tim J. Schulz, Yu-Hua Tseng, and C. Ronald Kahn

Obesity and body fat distribution are important risk factors for the development of type 2 diabetes and metabolic syndrome. Evidence has accumulated that this risk is related to intrinsic differences in behavior of adipocytes in different fat depots. In the current study, we demonstrate that adipocyte precursor cells (APCs) isolated from visceral and subcutaneous white adipose depots of mice have distinct patterns of gene expression, differentiation potential, and response to environmental and genetic influences. APCs derived from subcutaneous fat differentiate well in the presence of classical induction cocktail, whereas those from visceral fat differentiate poorly but can be induced to differentiate by addition of bone morphogenetic protein (BMP)-2 or BMP-4. This difference correlates with major differences in gene expression signature between subcutaneous and visceral APCs. The number of APCs is higher in obesity-prone C57BL/6 mice than obesity-resistant 129 mice, and the number in both depots is increased by up to 270% by exposure of mice to high-fat diet. Thus, APCs from visceral and subcutaneous depots are dynamic populations, which have intrinsic differences in gene expression, differentiation properties, and responses to environmental/genetic factors. Regulation of these populations may provide a new target for the treatment and prevention of obesity and its metabolic complications. *Diabetes* 61:1691–1699, 2012

There are two main types of white adipose tissue (WAT) in humans and rodents—subcutaneous (SC) fat and visceral (intra-abdominal [Vis]) fat. These contribute differentially to disease risk. Accumulation of Vis adipose tissue is associated with adverse metabolic outcomes, whereas increased amounts of SC fat has been viewed as neutral or even beneficial in its metabolic effects (1–3). While part of this difference may be related to anatomical location with different patterns of venous drainage, over the past few years, it has become clear that these two types of WAT differ in their intrinsic characteristics, including levels of adipokine secretion, insulin sensitivity, lipolysis rate, and tendency to develop inflammation (4). We and others (5–7) recently have shown that this correlates with differences in gene expression between adipocytes in different depots, including the expression of fundamental development and patterning genes. Differences in differentiation and developmental gene

expression have also been observed in human preadipocytes from different depots (8), but exactly how this relates to intrinsic differences in adipose tissues and the propensity for obesity and insulin resistance is unclear.

Spalding et al. (9) recently demonstrated that in humans, ~10% of the adipocyte pool turns over annually and that the absolute number of adipocytes turning over in individuals with obesity is approximately double from that in lean individuals. Exactly how adipocytes in different depots turn over and to what extent this is influenced by genetic or environmental factors is unknown. However, using lineage tracing and fluorescence-activated cell sorting (FACS) strategies, two groups (10,11) have developed techniques to identify and isolate the adipocyte precursor cells (APCs) from the stromovascular fraction (SVF) of white fat. In the current study, we show that APCs are dynamic and respond to different environmental and genetic factors. We show that APCs from Vis versus SC fat differ in their specific gene expression signatures and that SC APCs are more adipogenic and require fewer growth factors, whereas Vis APCs have anti-adipogenic characteristics and require additional growth factor stimulation to differentiate. These results show that there are intrinsic differences between preadipocytes from different depots and that these differences contribute to the differential properties and turnover of adipocytes in different depots.

RESEARCH DESIGN AND METHODS

Mice. C57BL/6 mice and 129 mice were obtained from The Jackson Laboratory and kept under a normal diurnal cycle in a temperature-controlled room. Mice were fed with standard chow containing 22% of calories from fat (Mouse Diet 9F 5020; PharmaServ) or a 60% high-fat diet (HFD) (OpenSource Diet D12492; Research Diets). For the HFD versus chow diet study, two cohorts of mice were used starting at aged 3 and 8 weeks. Animal care and study protocols were approved by the animal care committee of Joslin Diabetes Center and were in accordance with National Institutes of Health guidelines.

Adipocyte precursor isolation and flow cytometry. Epididymal and inguinal fat pads, representing Vis and SC fat, respectively, were cut in small pieces and incubated with 1 mg/mL collagenase I for 30 min. The cell suspension was filtered through a 150- μ m nylon mesh, and the SVF was isolated by low-speed centrifugation. For FACS analysis, erythrocyte-free SVF cells were incubated with a mix of antibodies against different surface markers as described previously (10) and sorted using an Aria flow cytometer (BD Biosciences). Dead cells were removed using propidium iodide staining. Cells negative for Ter119, CD45, and CD31 and positive for both SCA1 and CD34 were considered as APCs.

Cell culture and differentiation of APCs. Cells were grown as described previously (12) with some modifications. Medium containing 60% Dulbecco's modified Eagle's medium–low glucose (Invitrogen) and 40% MCDB201 (Sigma-Aldrich) and supplemented with Normocin 0.1 mg/mL (InvivoGen), 10% FBS, 1 \times insulin-transferrin-selenium mix, 1 \times linoleic acid conjugated to BSA, 1 nmol/L dexamethasone, and 0.1 mmol/L L-ascorbic acid 2-phosphate (Sigma-Aldrich) was used as growth medium. This medium was further supplemented with 10 ng/mL epidermal growth factor (PeproTech), 10 ng/mL leukemia inhibitory factor (Millipore), 10 ng/mL platelet-derived growth factor BB (PeproTech), and 5 ng/mL basic fibroblast growth factor (Sigma-Aldrich). Once sorted, cells were rinsed with medium and plated at 50,000 cells per well in 24-well plates. After 6–7 days, cells reached ~80% confluence. Medium was changed every other day. For differentiation, cells were seeded at 20,000 cells per well in

From the Joslin Diabetes Center, Harvard Medical School, Boston, Massachusetts.

Corresponding author: C. Ronald Kahn, c.ronald.kahn@joslin.harvard.edu.

Received 19 December 2011 and accepted 5 March 2012.

DOI: 10.2337/db11-1753

This article contains Supplementary Data online at <http://diabetes.diabetesjournals.org/lookup/suppl/doi:10.2337/db11-1753/-DC1>.

Y.M. is currently affiliated with the Instituto de Neurobiología, Universidad Nacional Autónoma de México, Querétaro, Mexico.

© 2012 by the American Diabetes Association. Readers may use this article as long as the work is properly cited, the use is educational and not for profit, and the work is not altered. See <http://creativecommons.org/licenses/by-nc-nd/3.0/> for details.

48-well plates. After cells reached 80% confluence, they were treated or not for 2 days with 3.3 nmol/L BMP-2 or BMP-4 (R&D Systems) in growth medium with 2% FBS and without growth factors. Medium was then replaced by differentiation medium (growth medium with no growth factors but with 2% FBS, 1 μ mol/L dexamethasone, 0.5 μ mol/L isobutylmethylxanthine, 100 nmol/L insulin, and 1 μ mol/L rosiglitazone) for 3 days, after which the medium was replaced with growth medium containing 2% FBS and 100 nmol/L insulin for 2 more days; for the last 2–3 days of differentiation, cells were incubated with growth medium with 2% FBS alone.

RNA extraction and PCR. RNA was extracted from cells using RNeasy (QIAGEN). Reverse transcription was performed with 0.3 μ g RNA by using High Capacity cDNA Reverse Transcription Kit (Applied Biosystems, Foster City, CA). Real-time PCR was performed using Maxima SYBR Green (Fermentas, Glen Burnie, MD) in duplicate using the ABI Prism 7900 System (Applied Biosystems) under the following conditions: 50°C –2 min, 95°C –10 min, and 40 cycles of 95°C –15 s, 60°C –20 s, and 72°C –30 s. Dissociation protocols were conducted after every run to check for primer specificity. To obtain relative expression values, we calculated the $2^{-\Delta C_t}$ parameter for each individual sample using cycle threshold values of TATA-box-binding protein as an endogenous control.

Microarray. Approximately 1×10^6 sorted cells per sample were used to isolate RNA for the microarray analysis. Five independent RNA samples each from a pool of isolated APCs from 10 different mice from each depot were analyzed on Mouse Genome 430 2.0 arrays (Affymetrix, Santa Clara, CA). All data were subjected to global normalization to an intensity of 1,500 using the Gene Chip Software MAS V. 5.0. All differences reported had a P value <0.05.

RESULTS

Isolation of APCs from different WAT depots. APCs were isolated by FACS from SVFs of Vis and SC fat from mice as described above and in Supplementary Fig. 1. Cells negative for CD45, CD31, and Ter119 and positive for CD34 and SCA1 were considered APCs. Cells positive for CD45, CD31, and/or Ter119 (endothelial cells, platelets, macrophages, white blood cells, osteoclasts, and erythrocytes) were designated as “other SVF.” Only live cells were counted. In a typical sorting, using male C57BL/6 mice aged 8 weeks, Vis fat contained $0.9 \pm 0.1 \times 10^5$ APCs and $3.5 \pm 0.8 \times 10^5$ other SVF cells per fat pad, whereas SC fat contained $0.65 \pm 0.08 \times 10^5$ APCs and $7.1 \pm 0.7 \times 10^5$ other SVF cells per fat pad (Fig. 1A). Thus, the percentage of stromovascular cells, which are APCs, was almost three times higher in Vis fat than in SC fat (21 ± 3.7 vs. $7.8 \pm 1.7\%$) (Fig. 1B).

APCs from different fat depots differ in their differentiation requirements. To confirm that the isolated APCs were preadipocytes, we analyzed the differentiation ability of both Vis and SC APCs. Confluent APC cultures were treated with the typical induction protocol,

including rosiglitazone, and differentiation was assessed by lipid accumulation and expression of markers of terminal differentiation, including *Slc2a4* (Glut-4), *Adipoq* (adiponectin), *Lep* (leptin), and *Fabp4* (fatty acid binding protein or aP2). Using this approach, APCs from the SC fat differentiated well within 7 days after induction, with >90% of the cells containing large lipid droplets (Fig. 2A). In fact, ~10% of SC APCs differentiated in the absence of any hormonal induction (Fig. 2A). By contrast, with the same protocol, <20% of APCs from the Vis depot could be induced to differentiate (Fig. 2A). This raised two possibilities: one was that the Vis APCs were not really adipocyte precursors; the other was that the APCs were missing some signals required for differentiation.

BMPs are known to induce commitment of mesenchymal stem cells into adipocytes, muscle, and bone (13–15). We hypothesized that perhaps BMP signaling was lacking in the APCs from the Vis depot. We therefore pretreated subconfluent Vis and SC APCs with 3.3 nmol/L BMP-4 for 2 days prior to the addition of the induction cocktail (IC) and then assessed differentiation. With the SC APCs, BMP-4 pretreatment did not further enhance the almost complete differentiation achieved by the IC alone (Fig. 2A). However, with the Vis APCs, BMP-4 pretreatment markedly enhanced differentiation, resulting in almost 90% of cells showing typical lipid droplets (Fig. 2A). Pretreatment with BMP-2 induced Vis APCs to differentiate at a similar extent as BMP-4 (Fig. 2B) but had no further effect on SC APCs (not shown).

These differences in differentiation potential were confirmed by quantitative PCR analysis for expression of terminal adipocyte differentiation genes. SC APCs 7–8 days after treatment with standard IC with or without BMP-4 treatment showed marked increases in expression of *Fabp4* (730-fold), *Slc2a4* (300-fold), *Adipoq* (730-fold), and *Lep* (20-fold) (Fig. 2C, right three bars, each panel). On the other hand, Vis APCs treated with standard IC showed little accumulation of lipid and very small increases in expression of these differentiation markers (Fig. 2C, left two bars, each panel). However, when the Vis APCs were pretreated with BMP-4 followed by IC, the increases in gene expression were similar to those seen in SC APCs after differentiation, with large increases in *Fabp4* (480-fold), *Slc2a4* (160-fold), *Adipoq* (660-fold), and *Lep* (21-fold) (Fig. 2C, third bar, each panel).

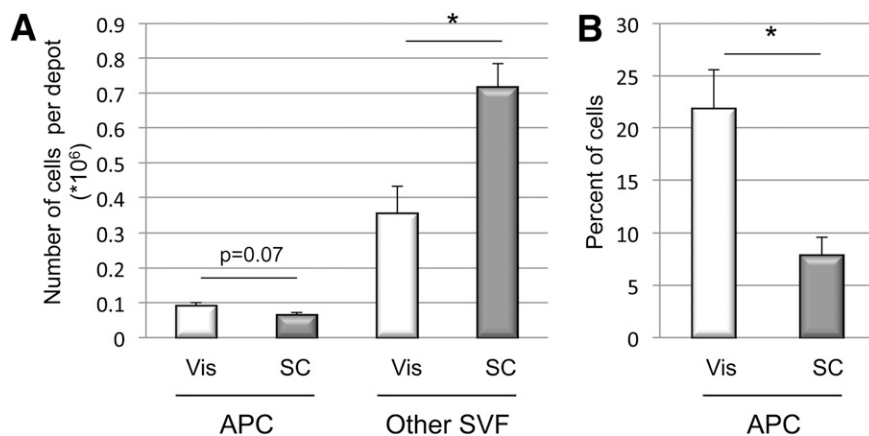


FIG. 1. Frequency of APCs and other SVF cells in SC vs. Vis depots. Typical FACS sorting analysis of APCs and other SVF cells from SC and Vis depots isolated from male mice aged 7–9 weeks. Data were calculated using only live cells. Double positive CD34, SCA1 (and CD45[−], CD31[−], and Ter119[−]) cells were considered APCs, whereas CD45⁺, CD31⁺, and Ter119⁺ cells were considered as other SVF cells. **A:** Number of cells per depot. **B:** Percent of APCs in both depots relative to other SVF cells. Data are mean \pm SEM of $n = 4$ independent experiments. Statistics were analyzed by Student t test (two-way, unequal variance). * $P < 0.05$.

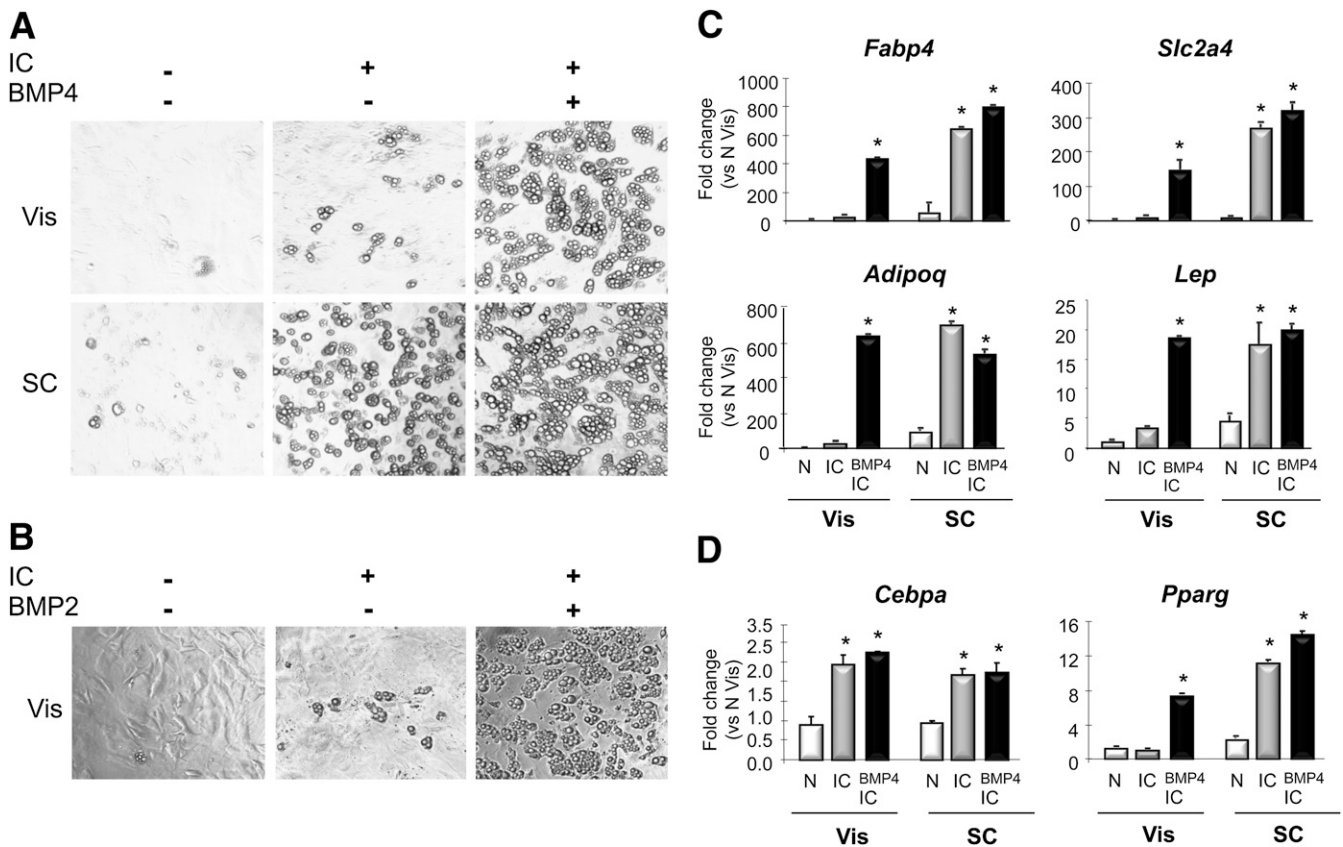


FIG. 2. Higher differentiation capacity in APCs from SC than from Vis depots. After FACS sorting, APCs from SC and Vis depots were placed in culture; upon 80% confluence, they were treated with or without BMP2 or BMP4 and 2 days later, were induced to differentiate (insulin, isobutylmethylxanthine, dexamethasone, and rosiglitazone). Seven days after induction of differentiation, they were photographed to evaluate for lipid-containing mature adipocytes (*A* and *B*) or lysed, mRNA extracted, and processed for quantitative PCR to evaluate expression changes on adipocyte differentiation genes (*C* and *D*). Graphs show fold changes vs. N Vis. N, control without BMPs or IC; BMP4 IC, BMP4 pretreatment followed by IC. Data are mean \pm SEM of $n = 2$ independent experiments. Statistics were analyzed by Student *t* test (two-way, unequal variance). * $P < 0.05$.

Gene expression analysis also indicated that the block in differentiation was at an early step involved in the stimulation of PPAR γ . Thus, standard IC increased expression of *Cebpa* by greater than twofold in APCs from both Vis and SC fat, and *Cebpa* was not further increased by BMP-4 pretreatment (Fig. 2D). On the other hand, in SC APCs, *Pparg* increased fivefold after differentiation using standard IC or BMP-4 plus IC. However, in Vis APCs, *Pparg* expression was not changed by treatment with IC but was increased sixfold when cells were pretreated by BMP-4 plus IC (Fig. 2D). Taken together, these data indicate that the block in differentiation in Vis APCs lies in the inability of standard induction hormones to trigger the expression of *Pparg* and induce the transcriptional events required for differentiation and that this block can be released by stimulation of the BMP pathway. Since C/EBP α and PPAR γ can regulate expression of each other in a positive feedback manner (16) and since *Cebpa* is induced by standard IC in Vis fat, the blockade appears to be in the ability of C/EBP α to stimulate a normal increase in PPAR γ .

Proadipogenic gene expression signature in SC APCs. To identify possible differences between adipocyte precursors isolated from SC and Vis depots that might contribute to altered differentiation and other properties of the adipocytes, we performed microarray analysis on freshly isolated SC and Vis APCs from 7- to 8-week-old mice. Consistent with their increased ability to differentiate, when compared with Vis preadipocytes, SC APCs

showed significantly higher expression of genes involved in positive regulation of adipocyte differentiation, including *Pparg* (3.2-fold), *Cebpa* (1.3-fold), the dickkopf homolog DKK2 (9.1-fold), *Stat5a* (2.9-fold), and the BMPs associated with WAT differentiation, *Bmp2* (1.5-fold) and *Bmp4* (1.5-fold) (all $P < 0.05$). By contrast, Vis APCs showed increased expression of genes that can act as inhibitors of adipocyte differentiation, including *Gata2* (7.4-fold) and *Tgfb2* (1.8-fold) (Table 1 and Supplementary Table 1). It is interesting that APCs from the Vis depot also expressed higher levels of markers found in bone marrow mesenchymal cells (17), including *Lif*, *Igf1*, *Igfbp7*, *Ctgf*, *Mgp*, *Trib2* and *Pgn1/Bgn* (Table 1).

Depot-specific gene expression signatures. We (5,6) and others (7,18,19) have previously shown that mature adipocytes from Vis and SC fat have different patterns of gene expression, including genes involved in adipocyte function and developmental patterning. Comparing the results from APCs in the current study with our previous results in mature adipocytes from mice, we could identify depot-specific signatures. These consisted of 19 genes that were much more highly expressed in the Vis depot and 32 genes that were much more highly expressed in the SC depot in both preadipocytes and adipocytes (Table 2).

Gene set enrichment analysis of the microarray data showed that SC APCs have increased expression in three major gene sets when compared with Vis APCs: 1) chemokines, 2) peptidases, and 3) proteins involved in the

TABLE 1
Pro- and anti-adipogenic gene expression signatures in Vis and SC APCs

	Fold	<i>P</i> value
Proadipogenic genes higher in SC APCs		
<i>Cepba</i>	1.3	0.03
<i>Pparg</i>	3.2	0.0001
<i>Dkk2</i>	9.1	0.0004
<i>Stat5a</i>	2.9	0.0001
<i>Bmp2</i>	1.5	0.001
<i>Bmp4</i>	1.5	0.02
Anti-adipogenic genes higher in Vis APCs		
<i>Gata2</i>	7.4	0.0005
<i>Tgfb2</i>	1.8	0.01
Bone marrow mesenchymal cell markers higher in Vis APCs		
<i>Lif</i>	2.46	0.039
<i>Igf1</i>	2.2	0.00008
<i>Igfbp7</i>	2.07	0.00004
<i>Ctgf</i>	4.29	0.003
<i>Mgp</i>	11.88	0.003
<i>Trib2</i>	1.75	0.047
<i>Pgn1/Bgn</i>	1.77	0.000003

vesicular fraction or microsomes (Table 2). In the Vis APCs, the most enriched gene sets fell into four major categories: 1) muscle related, with three related gene sets myofibril, sarcomere, and contractile fiber genes ($P < 0.02$); 2) monooxygenase activity; 3) developmental; and 4) negative regulation of cytokine biosynthesis (Table 3).

Genes most differentially expressed between Vis and SC APCs. The most differentially expressed gene, which was highly expressed in Vis APCs, was the transcription factor *Tcf21*, whereas in SC APCs, the most differentially expressed gene was the transcription factor *Lhx8* (LIM homeobox 8). Another interesting gene with significantly higher expression in SC versus Vis APCs was *Cd24*. This membrane protein was previously used as a surface marker (10) to isolate the APCs from a mixture of Vis and SC white fat depots. It is clear that this would result in preferential isolation of the SC APCs from this mixed fat cell pool. A heat map listing the 100 most differentially expressed genes is shown in Supplementary Fig. 2.

Effect of sex, strain, and age on adipocyte precursor frequency. To evaluate how the number of APCs and other SVF cells change between different genetic and environmental conditions, we analyzed APC frequency in young (2-month-old) versus old (1-year-old) mice, in obesity-prone (C57BL/6) versus obesity-resistant (129Sv/J) mice, and in male versus female mice. Aging altered dramatically the number of APCs. When expressed per gram of adipose tissue, APC numbers were twofold higher in young than in old mice in both depots (Fig. 3A). However, because fat mass increases with age, the total number of APCs per depot was increased by more than threefold in Vis and more than fourfold in SC fat in old versus young mice. The number of non-APCs (i.e., other SVF cells) per gram of fat was eightfold higher in SC fat of young versus old mice but similar in both age-groups in the Vis depot (Fig. 3A). However, the total number of other SVF cells per fat pad was almost sixfold higher in Vis fat of old versus young mice, while it remained similar in the SC depot between young and old mice. Therefore, when the number of APCs was calculated

as the percentage of total SVF cells in each depot, young mice had a significantly higher percentage of APCs than old mice in Vis fat (22 vs. 16%) but a smaller percentage of APCs in SC fat than old mice (3 vs. 13%) (Fig. 3A).

It is interesting that obesity-prone C57BL/6 mice already had almost twofold higher numbers of APCs per gram of fat than 129 mice in both depots by age 3 months. C57BL/6 mice also had ninefold more other SVF cells per gram of fat in the SC depot than 129 mice, whereas the number of other SVF cells in the Vis depot was similar. However, the percentage of APCs did not change between genotypes in Vis fat but was higher in the SC fat from 129 mice than in the same depot from C57BL/6 mice (17 vs. 4%) (Fig. 3B).

Between males and females, APCs and other SVF cells per gram of fat or per depot did not differ significantly. However, male mice did have a twofold higher number of other SVF cells in the Vis depot than female mice. As a result, the calculated percentage of APCs in the Vis depot (but not in the SC depot) from female mice was almost twice as high as that in males (29 ± 3 vs. $15 \pm 2\%$) (Fig. 3C).

Effect of HFD on adipocyte precursor frequency in young versus adult mice. Previous studies in humans show that early onset obesity is associated with adipocyte hyperplasia, whereas late onset of obesity is the result of adipocyte hypertrophy and hyperplasia; studies in rodents show hyperplasia can occur in both young and old animals (20–22). To determine if HFD-induced obesity might alter the number and percentage of APCs and other cells in the SVF at different ages, we used two experimental paradigms: one in which the HFD was started just after weaning (3 weeks old) and a second in which mice were started on the HFD as young adults (8–10 weeks old). As shown in Fig. 4A and B, APC number increased after 2 and 4 weeks on HFD in Vis and SC depots in both young and adult mice; however, the increase in APCs was larger when the mice were started on the HFD at a young age. Thus, Vis APC numbers increased by 80 and 60% after 2 and 4 weeks on HFD in young mice compared with 60 and 30% increases in adult mice. This difference was more marked in SC APCs, with 80 and 270% increases in cell numbers after 2 and 4 weeks on HFD in young mice compared with only 30 and 40% increases in adult mice. By contrast, the change in other SVF cells was greatest in the Vis depot but similar in young and adult mice, with increases of 210–270% in both young and adult mice on the HFD, whereas the number of other SVF cells in the SC depot increased modestly (60 and 70% for young and adult mice, respectively). Thus, HFD increases the number of other SVF cells only in the Vis depot, consistent with the increase in inflammatory cells in this compartment (23). When the percentage of APCs in the depot was calculated, the percentage of APCs increased by 250 and 180% after 2 and 4 weeks on HFD in young animals but was unchanged in adult animals. Thus, young prepubertal mice have an increase in APCs on HFD that is greater than that seen in adult animals, especially in the SC depot (Fig. 4).

DISCUSSION

Adipose tissue serves as an important regulator of metabolic homeostasis, and in this regard, not all fat is functionally equivalent. Thus, accumulation of Vis fat is associated with insulin resistance and a high risk for type 2 diabetes and metabolic syndrome, whereas accumulation of SC fat has been shown to have a possible protective value against these metabolic abnormalities. This appears to relate to

TABLE 2
Depot-specific signature of APCs and adipocytes from Vis and SC fat

Gene name	Gene symbol	Fold difference		Localization
		Adipo	Preads	
Depot-specific signature—Vis				
Angiotensinogen	<i>Agt</i>	7.5	5.8	Secreted
Aldo-keto reductase family 1, member C12	<i>Akr1c12</i>	2.6	6.9	Cytoplasm
AMP deaminase 3	<i>Ampd3</i>	2.5	2.8	Cytoplasm
Anillin, actin binding protein (scraps homolog, Drosophila)	<i>Anln</i>	5.3	2.8	Cytoplasm/Nucleus
Cysteine and glycine-rich protein 1	<i>Csrp1</i>	2.6	6.2	Nucleus
Cytochrome P450, family 1, subfamily b, polypeptide 1	<i>Cyp1b1</i>	11.0	3.2	ER/Mitochondria
Hydroxyprostaglandin dehydrogenase 15 (NAD)	<i>Hpgd</i>	2.2	2.0	Cytoplasm
Nuclear receptor subfamily 2, group F, member 1	<i>Nr2f1</i>	5.5	3.0	TF
Nuclear receptor subfamily 4, group A, member 1	<i>Nr4a1</i>	3.2	2.3	TF
Pterin 4 α carbinolamine dehydratase (TCF1) 1	<i>Pcbd1</i>	2.5	2.6	TF
Protocadherin 7	<i>Pcdh7</i>	2.6	2.1	PM
Plakophilin 2	<i>Pkp2</i>	2.9	2.8	PM
Prolactin receptor	<i>Prlr</i>	3.8	2.9	PM
Serum amyloid A3 pseudogene	<i>Saa3p</i>	2.6	5.2	Secreted
Solute carrier family 8, member 1	<i>Slc8a1</i>	2.3	4.2	PM
Secretory leukocyte peptidase inhibitor	<i>Slp1</i>	3.1	18.7	Secreted
Serine/arginine-rich protein specific kinase 2	<i>Srpk2</i>	2.2	2.2	Cytoplasm/Nucleus
Thrombospondin 1	<i>Thbs1</i>	5.8	3.6	Secreted
Transcription factor 21	<i>Tcf21</i>	3.0	216.2	TF
Depot-specific signature—SC				
Angiotensin-like 1	<i>Angptl1</i>	3.5	2.1	Secreted
Apolipoprotein D	<i>Apod</i>	3.8	2.0	Secreted
Chemokine (C-C motif) ligand 8	<i>Ccl8</i>	3.4	4.2	Secreted
Cadherin 2	<i>Cdh2</i>	2.9	2.5	PM
Cadherin 9	<i>Cdh9</i>	2.9	17.1	PM
Procollagen, type XII, α 1	<i>Col12a1</i>	3.4	3.4	Secreted
Procollagen, type I, α 1	<i>Col1a1</i>	4.7	3.3	Secreted
Early B-cell factor 3	<i>Ebf3</i>	2.0	4.1	TF
Engrailed 1	<i>En1</i>	8.0	4.5	TF
Estrogen receptor 1 (α)	<i>Esr1</i>	2.5	3.0	TF
Fibroblast growth factor 13	<i>Fgf13</i>	2.1	3.8	Secreted
Fibronectin type III domain containing 1	<i>Fndc1</i>	2.9	2.0	Secreted
Histocompatibility 2, Q region locus 10	<i>H2q10</i>	4.2	10.8	Membrane
Interferon- γ -inducible protein 47	<i>Ifi47</i>	4.0	2.8	ER/Membrane
Interferon- γ -induced GTPase	<i>Igtp</i>	2.0	2.4	Cytoplasm/Membrane
Interleukin-18 receptor 1	<i>Il18r1</i>	16.5	25.0	PM
Myelin basic protein	<i>Mbp</i>	3.9	9.1	Nucleus/Cytoplasm/IntMem
Matrix metalloproteinase 3	<i>Mmp3</i>	3.5	21.5	Secreted
Major urinary protein 1 /// major urinary protein 2	<i>Mup1/Mup2</i>	375.1	3.6	Secreted
Major urinary protein 3	<i>Mup3</i>	63.5	10.3	Secreted
Osteomodulin	<i>Omd</i>	3.8	2.4	Secreted
Procollagen C-endopeptidase enhancer protein	<i>Pcolce</i>	2.8	2.9	Secreted
Protein disulfide isomerase associated 5	<i>Pdia5</i>	5.9	2.1	ER
Serine (or cysteine) peptidase inhibitor, clade F, member 1	<i>Serpinf1</i>	2.9	2.0	Secreted
Secreted frizzled-related protein 2	<i>Sfrp2</i>	5.4	2.6	Secreted
Short stature homeobox 2	<i>Shox2</i>	8.7	95.4	TF
Sine oculis-related homeobox 4 homolog (Drosophila)	<i>Six4</i>	2.2	2.1	TF
ST6-N-acetylgalactosaminide α -2,6-sialyltransferase 5	<i>St6galnac5</i>	2.3	2.8	Golgi
T-box 15	<i>Tbx15</i>	12.2	145.4	TF
Transmembrane protein with EGF-like and 2 follistatin-like domains 2	<i>Tmeff2</i>	3.0	2.0	PM
Ubiquitin D	<i>Ubd</i>	5.7	2.3	Cytoplasm
Ubiquitin specific peptidase 18	<i>Usp18</i>	3.7	5.0	Cytoplasm

ER, endoplasmic reticulum; TF, transcription factor; PM, plasma membrane; IntMem, internal membrane.

intrinsic differences in the adipocytes in these fat depots (2,5,24–26). In the current study, we demonstrate that APCs from SC and Vis fat have important differences in terms of their gene expression signatures, their ability to differentiate, their response to growth factors, and their regulation in normal physiology and disease.

With regard to differentiation, previous studies show that SVF cells taken from SC fat of either rodents or humans differentiate more readily in culture than those from Vis fat (26–28). We show that the same is true for isolated APCs from these depots but find that this is because the APCs from SC and Vis depots have different differentiation

TABLE 3
Gene set enrichment analysis

Gene set	Gene symbol	Gene name	Fold change	P value
Enriched in Vis APCs				
Muscle related	<i>Des</i>	Desmin	5.5	0.000
Myofibril	<i>Tpm2</i>	Tropomyosin 2 (β)	3.6	0.020
Sarcomere	<i>Tpm1</i>	Tropomyosin 1 (α)	2.5	0.000
Contractile fiber	<i>Myoz2</i>	Myozenin 2	4.8	0.005
	<i>Tnni2</i>	Troponin T type 2	4.5	0.019
	<i>Tnni3</i>	Troponin I type 3	2.4	0.019
Monooxygenase activity	<i>Pah</i>	Phenylalanine hydrogenase	18.8	0.000
	<i>Fmo2</i>	Flavin containing monooxygenase 2	4.7	0.000
	<i>Cyp1b1</i>	Cytochrome P450 family 1 subfamily b	3.2	0.000
	<i>Cyp27a1</i>	Cytochrome P450 family 27 subfamily a	2.4	0.000
	<i>Fmo1</i>	Flavin containing monooxygenase 1	2.1	0.000
	<i>Cyp7b1</i>	Cytochrome P450 family 7 subfamily b	1.9	0.008
Developmental				
Mesoderm development	<i>Tcf21</i>	Transcription factor 21	216.2	0.000
	<i>Eya2</i>	Eyes absent homolog 2	4.9	0.003
	<i>Slit2</i>	Slit homolog 2	5.5	0.000
	<i>Mest</i>	Mesoderm specific transcript hom	1.6	0.010
Developmental maturation	<i>Rnd1</i>	ρ family GTPase 1	2.7	0.001
	<i>Ereg</i>	Epiregulin	1.9	0.015
	<i>Pick1</i>	Protein interacting with PRKCA1	1.4	0.006
	<i>Tgfb2</i>	Transforming growth factor, β 2	1.8	0.010
	<i>Myh11</i>	Myosin, heavy chain 11, s	1.9	0.040
Negative regulation of cytokine biology	<i>Inhbb</i>	Inhibin, β B	8.6	0.001
	<i>Inhba</i>	Inhibin, β A	3.9	0.000
	<i>Ela2</i>	Elastase 2	2.5	0.001
	<i>Il6</i>	Interleukin 6	1.8	0.001
Enriched in SC APCs				
Chemokines	<i>Cxcl9</i>	Chemokine (C-C motif) ligand 9	5.3	0.001
Chemokine activity	<i>Cxcl14</i>	Chemokine (C-X-C motif) ligand 14	4.2	0.002
Chemokine receptor binding	<i>Ccl8</i>	Chemokine (C-C motif) ligand 8	4.2	0.000
	<i>Cxcl13</i>	Chemokine (C-X-C motif) ligand 13	5.4	0.007
	<i>Cxcl10</i>	Chemokine (C-X-C motif) ligand 10	1.9	0.000
	<i>Ccl22</i>	Chemokine (C-C motif) ligand 22	5	0.007
Peptidase activity				
Cysteine type endopeptidase activity	<i>Lgmn</i>	Legumain	2.8	0.001
	<i>Casp9</i>	Caspase 9	2.8	0.003
	<i>Ctsk</i>	Cathepsin K	1.7	0.000
	<i>Casp1</i>	Caspase 1	1.9	0.009
	<i>Usp7</i>	Ubiquitin specific peptidase	1.7	0.001
	<i>Uchl1</i>	Ubiquitin carboxyl-terminal	1.3	0.010
	<i>Ctsb</i>	Cathepsin B	1.2	0.002
Aminopeptidase activity	<i>Trhde</i>	TRH-degrading enzyme	10.2	0.000
	<i>Lnpep</i>	Leucyl/cystinyl aminopeptidase	1.5	0.018
	<i>Anpep</i>	Alanyl (membrane) aminopeptidase	1.8	0.020
Vesicular fraction	<i>Stx16</i>	Syntaxin 16	1.9	0.007
Microsome	<i>Mgst3</i>	Microsomal glutathion S-transferase 3	1.7	0.001
	<i>Oas2</i>	2'-5'-oligoadenylate synthetase 2	2.2	0.03
	<i>Ltc4s</i>	Leukotriene C4 synthase	4.5	0.04
	<i>Ero1L</i>	ERO1-like	1.4	0.02
	<i>Slc35b1</i>	Solute carrier family 35, member b1	1.3	0.02
	<i>Sts</i>	Steroid sulfatase	1.3	0.01
	<i>Tmed2</i>	Transmembrane emp24 domain trafficking protein 2	1.4	0.01
	<i>Copa</i>	Coatomer protein complex subunit a	1.5	0.001

requirements. While SC APCs differentiate well using the standard IC, Vis APCs differentiate very poorly under the same conditions. However, pretreatment of Vis APCs with BMP-4 or BMP-2 allows these cells to undergo full differentiation. BMP-2 and BMP-4 have been shown to be required for commitment of the mesenchymal stem cell line

C3H10T1/2 to an adipocyte lineage (29), whereas committed cell lines, such as 3T3-L1, do not have this requirement. Indeed, Vis APCs are more like mesenchymal stem cells and less committed to adipocyte differentiation than cells bearing the same surface markers from SC fat. Vis APCs also show higher levels of expression of *Gata2*

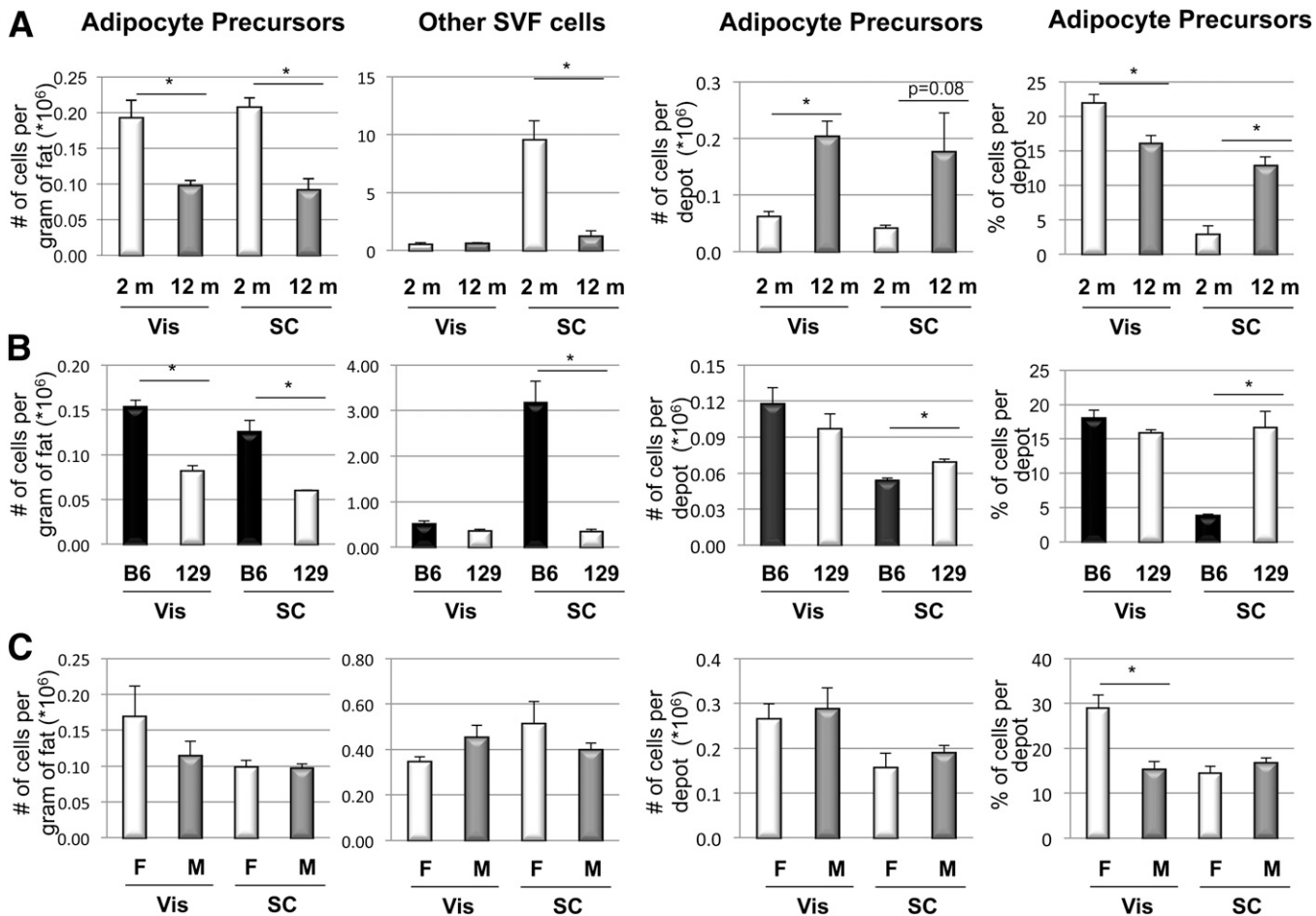


FIG. 3. Genetic and environmental impact on number (#) and percentage (%) of APCs and other SVF cells from Vis and SC fat depots. FACS sorting analysis of Vis and SC APCs and other SVF cells. Data were calculated using only live cells. Double positive CD34⁺, SCA1 (and CD45⁻, CD31⁻, and Ter119⁻) cells were considered APCs, whereas CD45⁺, CD31⁺, and Ter119⁺ cells were considered as other SVF cells. **A:** 8-week-old vs. 1-year-old C57BL/6 mice. m, month. **B:** C57BL/6 (B6) vs. 129 mice (3 months old). **C:** C57BL/6 male (M) vs. female (F) mice (6 months old). Five mice per group were used in two independent experiments. Data are mean \pm SEM. Statistics were analyzed by Student *t* test (two-way, unequal variance). **P* < 0.05.

and *Tgfb2*, factors known to inhibit adipogenesis (23,30), as well as higher levels of expression of mesenchymal stem cell markers (*Lif*, *Ctgf*, and *Mgp*), whereas SC APCs show higher expression of proadipogenic genes (*Pparg*, *Cebpa*, *Bmp2*, *Bmp4*, and *Dkk2*). Thus, Sca1⁺ and CD34⁺ SC APCs are more committed to the adipocyte lineage than Vis APCs expressing the same markers and have fewer requirements for becoming mature adipocytes.

At a cellular level, this difference in differentiation is due to a blockade in the ability of the IC to stimulate expression of *Pparg*. Thus, after treatment with IC, including the PPAR γ agonist rosiglitazone, Vis APCs show increased *Cebpa* but a failure of induction of *Pparg* and downstream adipogenic markers. BMP-2 and BMP-4 signals overcome the block and induce differentiation in Vis APCs. This may be in part because SC APCs already have enough endogenous BMP to trigger cell commitment, or it may depend on other differences between the two adipocyte precursor types. BMPs have been shown to induce *Pparg* through activation of schnurri-2, which forms a transcriptional complex with C/EBP α and SMAD1/4 (31). However, we find no difference in the level of schnurri-2 (Hivep2) between Vis and SC fat. In any case, in the presence of BMP-2, BMP-4, and IC, almost all of the Lin⁻, CD34⁺, and SCA1⁺ cells isolated from both Vis and SC depots are able to become adipocytes,

indicating the isolated APCs from both depots do represent the preadipocyte pool. This resistance to differentiation may explain why Vis fat expansion during adulthood occurs mainly by hypertrophy, whereas SC fat expansion is due primarily to hyperplasia (32).

Although others have analyzed differences in gene expression between Vis and SC adipose tissue (5,19,33), ours is the first study to identify genes that are differentially expressed between APCs in different depots. *Tcf21* is the most differentially expressed gene between Vis and SC adipocyte precursors, with the higher levels in Vis cells. This transcription factor also shows higher expression in mature adipocytes of Vis fat (34). While *Tcf21* has been described (34) as a marker for white preadipocytes compared with brown preadipocytes and muscle, in this study, preadipocytes were isolated only from epididymal fat, which have much higher expression than SC preadipocytes. The levels of *Tcf21* in SC preadipocytes are similar to those in brown preadipocytes and muscle.

The most differentially expressed gene in SC APCs is the LIM homeobox gene *Lhx8*. This gene had been previously described as a marker for brown preadipocytes when epididymal fat was the only source of WAT (34). However, *Lhx8* is not unique to brown preadipocytes but also a strong marker for SC preadipocytes (162-fold higher than in Vis

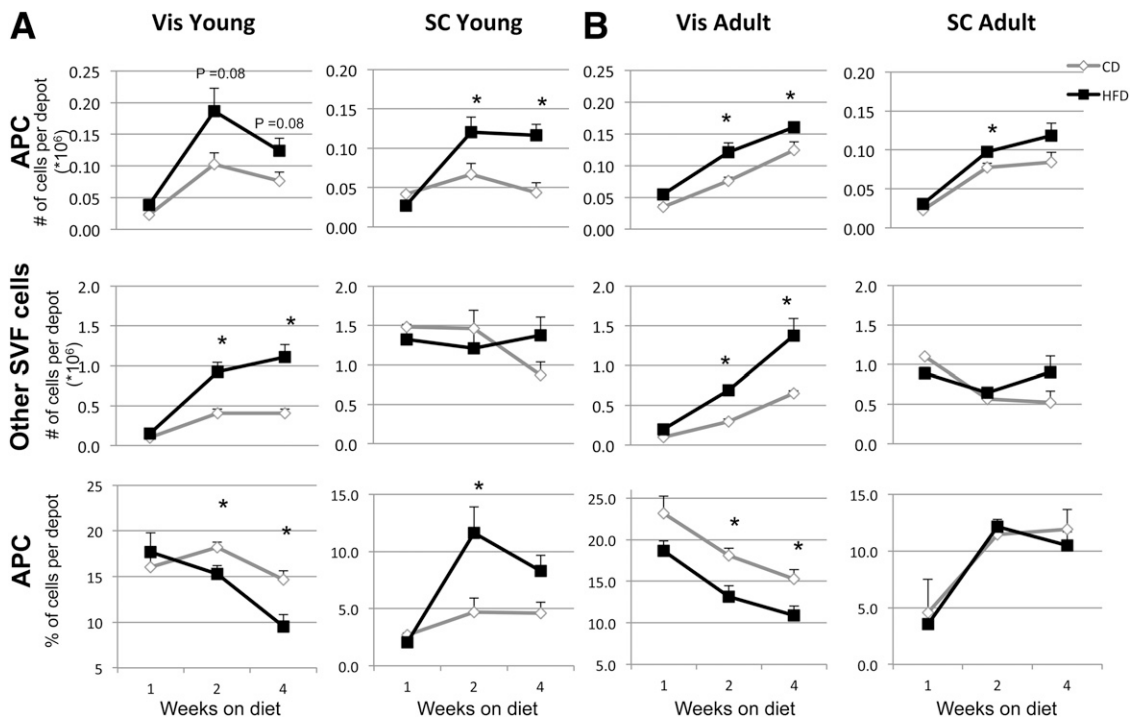


FIG. 4. Effect of HFD on number (#) and percentage (%) of APCs and other SVF cells from Vis and SC fat depots. FACS sorting analysis of Vis and SC APCs and other SVF cells. Data were calculated using only live cells. Double positive CD34, SCA1 (and CD45⁻, CD31⁻, and Ter119⁻) cells were considered APCs, whereas CD45⁺, CD31⁺, and Ter119⁺ cells were considered as other SVF cells. FACS sorted cells from mice placed on chow diet (CD) or HFD for 1, 2, and 4 weeks starting at age 4 weeks (A) or 8 weeks (B). Three to five mice per group were used in two independent experiments. Data are mean \pm SEM. Statistics were analyzed by Student *t* test (two-way, unequal variance). **P* < 0.05.

APCs). Thus, the pattern of gene expression in SC white fat has several similarities with that of brown fat, as compared with Vis white fat. Another gene more highly expressed in SC APCs than in Vis precursors is *Cd24*. This membrane protein was previously used as a marker (10) to purify the APCs but should probably not be used unless one is attempting to separate different populations from a mixture of white fat depots.

Our study also shows the dynamic nature of the adipocyte precursor pool. We find that HFD increases the number of APCs in both Vis and SC depots by as much as 270%. The increase is bigger when animals are started on HFD at a young age compared with when challenged as adults. Joe et al. (32) reported a similar increase in bromodeoxyuridine labeling of APCs in SC fat but a much smaller increase in labeling of Vis fat after 60 days of HFD. Whether this reflects differences in methodology, age of the mice, and a longer period of HFD is unknown.

Another difference between depots after challenge with HFD is that the number of non-APCs in the Vis depot increases dramatically after 2–4 weeks on HFD, whereas the number of other SVF cells in the SC depot remains constant. This causes a dramatic change in the relative proportion of cell types in these depots. Thus, the percentage of APCs in Vis fat decreases in mice on HFD compared with those on chow diet, whereas the percentage of APCs in the SC depot either increases or remains constant. This could explain why SC fat stays metabolically fit in obesity, whereas Vis fat develops inflammation, contributing to insulin resistance.

Fat mass increases with age, as does the number of APCs per depot, by three- to fourfold or more. As with HFD, however, the number of other SVF cells also increases,

especially in Vis fat. While sex has no effect on number of APCs in the SC depot, females show a trend to increased APCs and lower other SVF cells per gram of fat in Vis fat. This could reflect a reduced number of macrophages in the Vis depot of female mice and account for the higher insulin sensitivity of adipocytes from Vis fat of females compared with those from males (35).

Finally, the potential for new adipocytes also parallels the genetic risk for obesity. Thus, the obesity-prone C57BL/6 mouse has approximately twofold more APCs per gram of fat than the obesity-resistant 129 mouse by age 3 months. In adult animals, this is accompanied by increased content of lymphocytes and macrophages and expression of proinflammatory genes in Vis fat of C57BL/6 mice, contributing further to the tendency of C57BL/6 mice to develop insulin resistance upon aging or HFD-induced obesity (36).

In conclusion, APCs from Vis and SC depots differ dramatically in terms of their differentiation ability, gene expression signatures, growth factor requirements, and capacity to expand upon genetic and environmental stimuli. SC APCs are more committed to differentiate, whereas those from Vis depots have an anti-adipogenic profile and require growth factors, such as BMP-2 or BMP-4, to undergo differentiation. This helps explain why SC fat expands more by hyperplasia, whereas Vis fat expands by hypertrophy. These depot-specific gene signatures can serve as a powerful tool to identify and manipulate specific characteristics in the differentiation and functional properties of adipocytes and ultimately should help us understand how these two fat depots have opposing contributions to the development of diabetes and metabolic syndrome.

ACKNOWLEDGMENTS

This work was supported by National Institutes of Health Grant R01-DK-082659 and the Mary K. Iacocca Professorship. The study was also facilitated by support from the Joslin Diabetes and Endocrinology Research Center Core Laboratories (DK-036836). Y.M. was supported by the Pew Latin American Fellows Program in the Biological Sciences, the Mentor-Based American Diabetes Association Grant Award, and the Mexican Council of Science (CONACyT) Postdoctoral Fellowship. C.R.K. was supported by a grant from the Loveman Foundation.

No potential conflicts of interest relevant to this article were reported.

Y.M. conceived and designed the experiments, researched data, and wrote the manuscript. B.E. researched data, contributed to discussion, and reviewed and edited the manuscript. M.A.M. and S.G. researched data and reviewed and edited the manuscript. T.J.S. set up the methodology, contributed to discussion, and reviewed and edited the manuscript. Y.-H.T. contributed to discussion and reviewed and edited the manuscript. C.R.K. conceived and designed the experiments, reviewed the data, and wrote the manuscript. C.R.K. is the guarantor of this work and, as such, had full access to all the data in the study and takes responsibility for the integrity of the data and the accuracy of the data analysis.

Parts of this study were presented in abstract form at the 70th Scientific Sessions of the American Diabetes Association, Orlando, Florida, 25–29 June 2010.

The authors thank Joyce LaVecchio, Giri Buruzula, and the Flow Cytometry core for help with cytometry; Joshua Schroeder and the Genomics core for microarray processing; Michael Rourk and Graham Smyth for their expertise in animal care; and Madelana Basile and Jen Davison for editing the manuscript (all from Joslin Diabetes Center).

REFERENCES

- Misra A, Garg A, Abate N, Peshock RM, Stray-Gundersen J, Grundy SM. Relationship of anterior and posterior subcutaneous abdominal fat to insulin sensitivity in nondiabetic men. *Obes Res* 1997;5:93–99
- Snijder MB, Dekker JM, Visser M, et al. Associations of hip and thigh circumferences independent of waist circumference with the incidence of type 2 diabetes: the Hoorn Study. *Am J Clin Nutr* 2003;77:1192–1197
- Tran TT, Yamamoto Y, Gesta S, Kahn CR. Beneficial effects of subcutaneous fat transplantation on metabolism. *Cell Metab* 2008;7:410–420
- Wajchenberg BL, Giannella-Neto D, da Silva ME, Santos RF. Depot-specific hormonal characteristics of subcutaneous and visceral adipose tissue and their relation to the metabolic syndrome. *Horm Metab Res* 2002;34:616–621
- Gesta S, Blüher M, Yamamoto Y, et al. Evidence for a role of developmental genes in the origin of obesity and body fat distribution. *Proc Natl Acad Sci U S A* 2006;103:6676–6681
- Yamamoto Y, Gesta S, Lee KY, Tran TT, Saadati P, Kahn CR. Adipose depots possess unique developmental gene signatures. *Obesity (Silver Spring)* 2010;18:872–878
- Cantile M, Procino A, D'Armiento M, Cindolo L, Cillo C. HOX gene network is involved in the transcriptional regulation of in vivo human adipogenesis. *J Cell Physiol* 2003;194:225–236
- Tchoukalova YD, Koutsari C, Votruba SB, et al. Sex- and depot-dependent differences in adipogenesis in normal-weight humans. *Obesity (Silver Spring)* 2010;18:1875–1880
- Spalding KL, Arner E, Westermark PO, et al. Dynamics of fat cell turnover in humans. *Nature* 2008;453:783–787
- Rodeheffer MS, Birsoy K, Friedman JM. Identification of white adipocyte progenitor cells in vivo. *Cell* 2008;135:240–249
- Tang W, Zeve D, Suh JM, et al. White fat progenitor cells reside in the adipose vasculature. *Science* 2008;322:583–586
- Schulz TJ, Huang TL, Tran TT, et al. Identification of inducible brown adipocyte progenitors residing in skeletal muscle and white fat. *Proc Natl Acad Sci U S A* 2011;108:143–148
- Ahrens M, Ankenbauer T, Schröder D, Hollnagel A, Mayer H, Gross G. Expression of human bone morphogenetic proteins-2 or -4 in murine mesenchymal progenitor C3H10T1/2 cells induces differentiation into distinct mesenchymal cell lineages. *DNA Cell Biol* 1993;12:871–880
- Bowers RR, Lane MD. A role for bone morphogenetic protein-4 in adipocyte development. *Cell Cycle* 2007;6:385–389
- Schulz TJ, Tseng YH. Emerging role of bone morphogenetic proteins in adipogenesis and energy metabolism. *Cytokine Growth Factor Rev* 2009;20:523–531
- Rosen ED, Hsu CH, Wang X, et al. C/EBPalpha induces adipogenesis through PPARgamma: a unified pathway. *Genes Dev* 2002;16:22–26
- Igarashi A, Segoshi K, Sakai Y, et al. Selection of common markers for bone marrow stromal cells from various bones using real-time RT-PCR: effects of passage number and donor age. *Tissue Eng* 2007;13:2405–2417
- Vohl MC, Sladek R, Robitaille J, et al. A survey of genes differentially expressed in subcutaneous and visceral adipose tissue in men. *Obes Res* 2004;12:1217–1222
- Tchkonina T, Lenburg M, Thomou T, et al. Identification of depot-specific human fat cell progenitors through distinct expression profiles and developmental gene patterns. *Am J Physiol Endocrinol Metab* 2007;292:E298–E307
- Salans LB, Cushman SW, Weismann RE. Studies of human adipose tissue. Adipose cell size and number in nonobese and obese patients. *J Clin Invest* 1973;52:929–941
- Hirsch J, Batchelor B. Adipose tissue cellularity in human obesity. *Clin Endocrinol Metab* 1976;5:299–311
- Lemonnier D. Effect of age, sex, and site on the cellularity of the adipose tissue in mice and rats rendered obese by a high-fat diet. *J Clin Invest* 1972;51:2907–2915
- Wu H, Ghosh S, Ferrard XD, et al. T-cell accumulation and regulated on activation, normal T cell expressed and secreted upregulation in adipose tissue in obesity. *Circulation* 2007;115:1029–1038
- Hauer H, Entenmann G. Regional variation of adipose differentiation in cultured stromal-vascular cells from the abdominal and femoral adipose tissue of obese women. *Int J Obes* 1991;15:121–126
- Lafontan M, Girard J. Impact of visceral adipose tissue on liver metabolism. Part I: heterogeneity of adipose tissue and functional properties of visceral adipose tissue. *Diabetes Metab* 2008;34:317–327
- Tchkonina T, Giorgadze N, Pirtskhalava T, et al. Fat depot-specific characteristics are retained in strains derived from single human preadipocytes. *Diabetes* 2006;55:2571–2578
- Prunet-Marcassus B, Cousin B, Caton D, André M, Pénicaud L, Casteilla L. From heterogeneity to plasticity in adipose tissues: site-specific differences. *Exp Cell Res* 2006;312:727–736
- Adams M, Montague CT, Prins JB, et al. Activators of peroxisome proliferator-activated receptor γ have depot-specific effects on human preadipocyte differentiation. *J Clin Invest* 1997;100:3149–3153
- Bowers RR, Kim JW, Otto TC, Lane MD. Stable stem cell commitment to the adipocyte lineage by inhibition of DNA methylation: role of the BMP-4 gene. *Proc Natl Acad Sci U S A* 2006;103:13022–13027
- Tong Q, Dalgin G, Xu H, Ting CN, Leiden JM, Hotamisligil GS. Function of GATA transcription factors in preadipocyte-adipocyte transition. *Science* 2000;290:134–138
- Jin W, Takagi T, Kanesashi SN, et al. Schnurri-2 controls BMP-dependent adipogenesis via interaction with Smad proteins. *Dev Cell* 2006;10:461–471
- Joe AW, Yi L, Even Y, Vogl AW, Rossi FM. Depot-specific differences in adipogenic progenitor abundance and proliferative response to high-fat diet. *Stem Cells* 2009;27:2563–2570
- Atzmon G, Yang XM, Muzumdar R, Ma XH, Gabrieli I, Barzilai N. Differential gene expression between visceral and subcutaneous fat depots. *Horm Metab Res* 2002;34:622–628
- Timmons JA, Wennmalm K, Larsson O, et al. Myogenic gene expression signature establishes that brown and white adipocytes originate from distinct cell lineages. *Proc Natl Acad Sci U S A* 2007;104:4401–4406
- Macotela Y, Boucher J, Tran TT, Kahn CR. Sex and depot differences in adipocyte insulin sensitivity and glucose metabolism. *Diabetes* 2009;58:803–812
- Mori MA, Liu M, Bezy O, et al. A systems biology approach identifies inflammatory abnormalities between mouse strains prior to development of metabolic disease. *Diabetes* 2010;59:2960–2971